

Analytical canonical partition function of a quasi-one dimensional system of hard disks

V.M. Pergamenschik^{1,*}

¹*Institute of Physics, prospekt Nauky, 46, Kyiv 03039, Ukraine*

(Dated: October 15, 2020)

The exact canonical partition function of a hard disk system in a narrow quasi-one dimensional pore of given length and width is derived analytically in the thermodynamic limit. As a result the many body problem is reduced to solving single transcendental equation. The pressures along and across the pore, distributions of contact distances along the pore and disks' transverse coordinates are found analytically and presented in the whole density range for three different pore widths. The transition from the solidlike zigzag to liquidlike state is found to be quite sharp in the density scale but shows no genuine singularity. This transition is quantitatively described by the distribution of zigzag's windows through which disks exchange their positions across the pore. The windowlike defects vanish only in the densely packed zigzag which is in line with a continuous Kosterlitz-Thouless transition.

*email: victorpergam@yahoo.com

This paper is published in **J. Chem. Phys.** **153**, 144111 (2020);
<https://doi.org/10.1063/5.0025645>

INTRODUCTION

Over more than a century the idea to model molecules as hard spheres has been widely used in the theory of liquids [1–3]. In spite of apparent simplicity, the behavior of hard sphere systems is so complex mathematically that no exact analytical result has been obtained in 3 and even in 2 dimensions (2D). Under these circumstances, the numerical Monte Carlo and molecular dynamics approaches have become the main tools in the study of 3D hard sphere and 2D hard disk (HD) systems. The numerical results however are restricted to systems of a finite number of particles whereas such effects as, for instance, phase transitions, are related to systems in the thermodynamic limit when the number of particles N is infinite. As this limit can be studied only theoretically, analytical results are of great importance. The study of hard sphere systems is not restricted to their statistical equilibrium. Nowadays this system is also considered as a useful model glass former, and much efforts in this area have been devoted to analytical solutions in high unphysical and even infinite dimensions in a hope to get an insight into hard sphere systems in physical dimensions 2 and 3 (for instance, recent paper [4] and review [5]). But to attack the real dimensions directly is very difficult. The first exact analytical result was obtained in 1936 by Tonks for the purely 1D system of HDs. This system is much simpler than any 2D system, nevertheless Tonks' solution has become the analytical platform for further expansion into the world of 2D HD systems via moving to certain quasi-1D models. Barker was the first to point to the general possibility that the 1D case is amenable to a solvable generalization to quasi-1D case of HDs in narrow pores [7]. The simplest quasi-1D system (from now on just q1D) is such that each disk can touch no more neighbors than one from both sides (the so-called single-

file system); the width of such q1D pore must be below $\sqrt{3}/2 + 1$ times HD diameter. The analytical theory of HDs in q1D pore was presented by Wojciechowski et al [8] and ten years later was further developed by Kofke and Post [9]. Kofke and Post have elegantly shown that the problem can be reduced to solving certain integral equation. In general however the integral equation of this, now known as the transfer matrix method, cannot be solved analytically. A density expansion [10] and simplified model [11] to approximately solve this equation analytically have been proposed. The peculiarity of this method is that it is essentially related to the pressure-based (N, P, T) ensemble which does not directly predict pressure as a function of the system's width D and length L . In pursuit of an analytical result, the virial expansion for a q1D HD system has also been developed up to the fourth term [12]. In this paper I present exact analytical derivation of the canonical (N, L, D, T) partition function (PF) in the thermodynamic limit. As a result, finding the thermodynamic properties of a q1D HD system for given L and D is reduced to solving single transcendental equation which can be easily done numerically. The PF, pressure along and across the pore, distribution of the contact distances between neighboring HDs along the pore, and distribution of HD centers across the pore are found analytically; the constant to be found numerically fully specifies the PF and these distribution functions. The longitudinal and transverse pressures and the above distributions are presented for three pore widths in the total range of linear density $\rho = N/L$. The disks' arrangement for different densities N/L is discussed.

The developed analytical theory enables for a deeper insight into the transition from solidlike to liquidlike state in a q1D HD system. The system shows a sharp crossover, but the thermodynamics does not show any genuine discontinuity. We found that this is similar to the

melting in a continuous Kosterlitz-Thouless-type transition. A solid-to-fluid transition is a global phenomenon attributed to the entire body, but in a 2D crystals it starts from local emergence of bounded defect pairs [13]. The densely packed state of a q1D system is the zigzag array where all disks are caged and cannot move across the pore. To gain entropy the system searches for uncaging. Though uncaging cannot occur in the entire system, it can occur locally where pair of disks tries to exchange their positions across the pore. Usually, the density of defects is determined by their core energy via Boltzmann's factor, but in our case it is irrelevant as possible defects have a purely entropic origin. The distribution of contact distances along the pore gives the rate of such entropic defects. As density decreases, it predicts an emergence of progressively larger number of windowlike defects in the zigzag arrangement. These windows are of the size of disk diameter so that through them pairs of disks can exchange their position across the pore. The number of these defects vanishes only in the densely packed state which is in line with a continuous Kosterlitz-Thouless-type transition. The similarity has been strongly supported by the results on the correlation decay in a q1D HD system recently obtained by molecular dynamics simulation in [14, 15]. Note that defects of the zigzag arrangement, which are similar to our windowlike defects, in connection with their role in the disk motion across the pore have been discussed earlier in [4, 16].

PARTITION FUNCTION

Consider a pore of the width D and length L filled with N HDs of diameter $d = 1$, Fig.1. We assume the thermodynamic limit $N \rightarrow \infty, L \rightarrow \infty$ while $N/L = \text{const}$; the terms which vanish in this limit (e.g., the end effects) will be omitted. All lengths will be measured in HD diameters. The width parameter $\Delta = (D - d)/d$, that gives the actual pore width attainable to HD centers, in the quasi 1D case ranges from 0 in the 1D case to the maximum $\sqrt{3}/2 \approx 0.866$. The i -th disk has two coordinates, x_i along and y_i across the pore; y varies in the range $-\Delta/2 \leq y \leq \Delta/2$; the pore volume is LD . The vertical center-to-center distance between two neighbors, $\delta y_i = y_{i+1} - y_i$, determines the contact distance σ_i between them along the pore:

$$\begin{aligned} \sigma_i &= \min |x_{i+1}(y_{i+1}) - x_i(y_i)|, \\ \sigma_i &= \sqrt{d^2 - \delta y_i^2}, \\ \sigma_m &= \sqrt{d^2 - \Delta^2} \leq \sigma \leq d = 1. \end{aligned} \quad (1)$$

The minimum possible σ, σ_m , obtains for $\delta y = \pm\Delta$ when the two disks are in contact with the opposite walls. Thus, each set of coordinates $\{y\} = y_1, y_2, \dots, y_N$ determines the correspondent densely

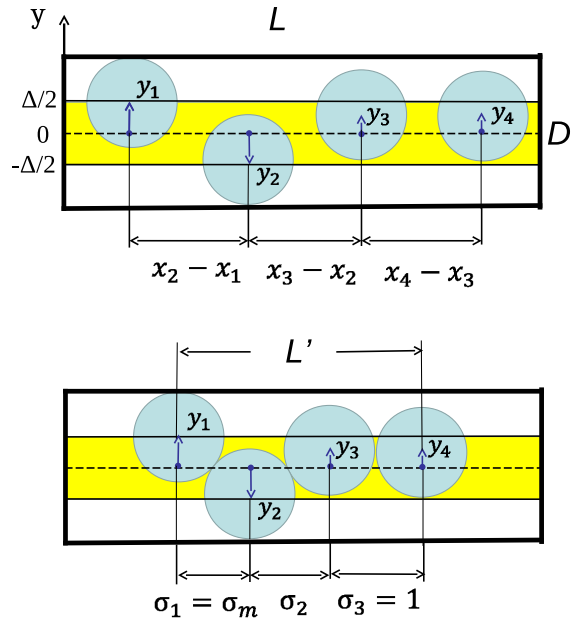


FIG. 1: Four HDs in the $L \times D$ pore and the condensate (below) correspondent to their vertical coordinates $\{y\}$. The inner fraction of thickness Δ is the volume accessible to disks' centers. The end effect in L' (one diameter d compared to L') is neglected.

packed state of the total length $L'\{y\} = \sum_{i=1}^{N-1} \sigma_i(\delta y_i)$, Fig. 1, which we call condensate and which plays the central role in our theory. The minimum condensate length is $\sigma_m N$, the maximum length can be as large as Nd , but it cannot exceed L : $N\sigma_m < L' \leq L'_{\max}$ where $L'_{\max} = \min(Nd, L)$.

In this paper we will systematically use singular functions and their analytical representations as this substantially simplifies both the integration domains and calculation of the manifold integrals. We will use the notation $D^{N-1}x = dx_1 \dots dx_{N-1}$ for the product measure. Omitting unimportant factors, the exact configurational canonical (N, L, D) PF of the q1D HD system has the following form:

$$\begin{aligned} Z &= \int_{-\Delta/2}^{\Delta/2} D^N y \times \theta \left(L'_{\max} - \sum_{i=1}^{N-1} \sigma_i \right) \\ &\times \theta \left(\sum_{i=1}^{N-1} \sigma_i - (N-1)\sigma_m \right) \int_X D^N x, \end{aligned} \quad (2)$$

where θ is the step-function: $\theta(x) = 1$ for $x \geq 0$ and $\theta(x) = 0$ otherwise. The x integration domain X was first formulated by Tonks [6] for the 1D case and much

later by Wojciechowski et al [8] for a q1D system:

$$\int_X D^N x = \int_{d/2}^{x_2-\sigma_1} dx_1 \int_{\sigma_1+d/2}^{x_3-\sigma_2} dx_2 \dots \int_{\sum_{i=1}^{N-2} \sigma_i+d/2}^{L-d/2} dx_N \quad (3)$$

For all y coordinates fixed, X ensures that under the single-file condition the disks do not intersect: disk i can move between two next neighbors $i-1$ and $i+1$, its minimum distance to disk $i-1$ is $\sigma_{i-1}(\delta y_{i-1})$ and that to disk $i+1$ is $\sigma_i(\delta y_i)$, and so on; the minimum distance between disks 1 and N and the correspondent walls is $d/2$. We start with resorting to the alternative form of integral (3) in which the integration domain is fixed by a theta function. To this end we change from the variables x_1, x_2, \dots, x_N to variables $x_1, \delta x_1, \delta x_2, \dots, \delta x_{N-1}$ where $\delta x_i = x_{i+1} - x_i$; the Jacobian of this well-known change of variables is 1. Then the x integral takes the following form:

$$\int_X D^N x = \int_0^{L-d-\sum_{i=1}^{N-1} \sigma_i} \frac{dx_1}{N!} \times \int_0^{L-d-\sum_{i=1}^{N-1} \sigma_i} D^{N-1} \delta x \theta \left(L - \sum_{i=1}^{N-1} \delta x_i \right). \quad (4)$$

The theta fuction $\theta(L - \sum \delta x_i)$ restricts the x integration to those x for which the condensate's length does not exceed the total length L ; as each $\delta x(\delta y)$ is restricted by its lower boundary $\sigma(\delta y)$ the disks cannot overlap. As the integrarion limits in all δx are the same, the factor $1/N!$ is needed to exclude permutations of the x coordinates which were precluded in the original integral (3) by the form of the integration domain. The analytical form of the theta function is

$$\theta(x) = \frac{1}{2\pi} \int_{-\infty}^{\infty} \frac{d\alpha}{i\alpha} e^{i\alpha x}, \quad (5)$$

where the integration path circumvents the point $\alpha = 0$ from below. We make use of this formula in (4) and perform the δx integration to get

$$\int_X D^N x = \int_0^{L-d-\sum_{i=1}^{N-1} \sigma_i} \frac{dx_1}{N!} \int_{-\infty}^{\infty} \frac{d\alpha}{2\pi i\alpha} e^{i\alpha L} \times \left[\frac{\exp i\alpha \left(L - d - \sum_{i=1}^{N-1} \sigma_i \right) - 1}{i\alpha} \right]^{N-1}. \quad (6)$$

The α integrand has a pole at $\alpha = 0$ which is of the first order as the expression in the square brackets is regular

at this point. Taking the residue and performing the x_1 integration one finally obtains:

$$\int_X D^N x = \frac{1}{N!} \left(L - d - \sum_{i=1}^{N-1} \sigma_i \right)^N. \quad (7)$$

In the 1D case, all σ 's are equal to d and this expression is the PF obtained by Tonks:

$$Z_{1D} = \frac{1}{N!} (L - Nd)^N. \quad (8)$$

Let us proceed with the PF (2). Substituting (7) and changing from the variables y_1, y_2, \dots, y_N to the variables $y_1, \delta y_1, \dots, \delta y_{N-1}$ one gets:

$$Z = \int_{-\Delta}^{\Delta} D^{N-1} \delta y \left(L - \sum_{i=1}^{N-1} \sigma_i \right)^N \times \theta \left(L'_{\max} - \sum_{i=1}^{N-1} \sigma_i \right) \theta \left(\sum_{i=1}^{N-1} \sigma_i - (N-1)\sigma_m \right). \quad (9)$$

The θ functions restrict the y integration domain to those $\{y\}$ for which σ 's are in the allowed range, $\sigma_m \leq \sigma_j(\delta y_j) \leq 1$, but their sum does not exceed L'_{\max} . However, rather than integrating over the entire δy domain defined by the θ function, it is convenient first to fix the condensate's length at some L' and then integrate over its possible values. This can be done by introducing following representation of the step function θ :

$$\theta \left(L'_{\max} - \sum \sigma_j \right) \theta \left(\sum \sigma_i - (N-1)\sigma_m \right) = \int_{(N-1)\sigma_m}^{L'_{\max}} dL' \delta \left(L' - \sum \sigma_i \right), \quad (10)$$

where one diameter d is neglected in comparison to L . From now on we set $d = 1$. Next we change the integration over δy to that over σ , $d\delta y_i = d\tilde{\sigma}_i = \sigma_i d\sigma_i / \sqrt{1 - \sigma_i^2}$. Then, in the context of (10), Z becomes

$$Z = \int_{N\sigma_m}^{L'_{\max}} dL' (L - L')^N \int_{\sigma_m}^1 D^{N-1} \tilde{\sigma} \delta \left(L' - \sum \sigma_i \right). \quad (11)$$

We use the analytical representation of the delta function in Z :

$$\delta \left(L' - \sum \sigma \right) = \frac{1}{2\pi} \int_{-\infty}^{\infty} d\alpha e^{i\alpha(L' - \sum \sigma)}. \quad (12)$$

Next we perform the $\tilde{\sigma}$ integration which factorizes into $N-1$ similar integrals to obtain

$$Z = \int_{-\infty}^{\infty} d\alpha \int_{N\sigma_m}^{L'_{\max}} dL' e^{i\alpha L'} (L - L')^N \left(\int_{\sigma_m}^1 d\tilde{\sigma} e^{-i\alpha \sigma} \right)^{N-1}. \quad (13)$$

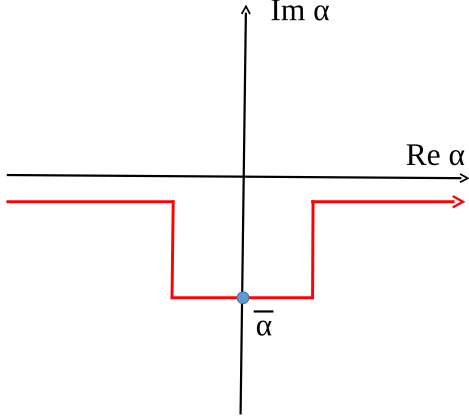


FIG. 2: The intergation contour over α deformed as to pass through the saddle point $\bar{\alpha}$. The length of the segment with this point is on the order of $1/\sqrt{N}$.

It is convenient to introduce the per disk lengths $l' = L'/N$, $l'_{\max} = L'_{\max}/N$, $l = L/N$ and rewrite the PF in the following form:

$$Z = \int_{\sigma_m}^{l'_{\max}} dl' \int d\alpha e^{Ns}, \quad (14)$$

where the factor N^N is omitted, $N - 1$ is replaced by N and

$$s = i\alpha l' + \ln(l - l') + \ln \left(\int_{\sigma_m}^1 d\tilde{\sigma} e^{-i\alpha\sigma} \right). \quad (15)$$

Now we can compute the PF (14) by the steepest descent method. It is convenient to introduce $a = i\alpha$ which is real since α at the saddle point lies on the imaginary axis and the integration contour has to be (and can be) properly deformed, Fig. 2. The saddle point in the limit $N \rightarrow \infty$ determines the integral (14) exactly. It is specified by the stationary point of the function s (15) which, for given l and σ_m , depends on a and l' . The two equations $\partial s/\partial a = \partial s/\partial l' = 0$ can be reduced to the single equation which reads:

$$\int_{\sigma_m}^1 d\sigma f_{\sigma}(\sigma, a)\sigma = \bar{\sigma}, \quad (16)$$

$$\bar{\sigma} = l - 1/a, \quad (17)$$

where we introduced the function

$$f_{\sigma}(\sigma, a) = \frac{\sigma e^{-a\sigma}}{\sqrt{1 - \sigma^2} \int_{\sigma_m}^1 \frac{d\sigma \sigma e^{-a\sigma}}{\sqrt{1 - \sigma^2}}}. \quad (18)$$

The solution \bar{a} of equation (16) depends on the per disk pore length l and, via σ_m , on the pore width D , and

fully determines the free energy. The free energy F per disk, which therefore is the function of the length l , width D , and the temperature T , is $F(l, D, T) = -Ts(\bar{a}) = -TS$ where S is system's per disk entropy (up to terms independent of L and D):

$$S = \bar{a}\bar{\sigma} + \ln(l - \bar{\sigma}) + \ln \left(\int_{\sigma_m}^1 \frac{d\sigma \sigma e^{-\bar{a}\sigma}}{\sqrt{1 - \sigma^2}} \right). \quad (19)$$

Finally, the PF has the form

$$Z = \exp(NS), \quad (20)$$

where the prefactor $\sim \sqrt{N}$ is omitted since in the thermodynamic limit its contribution is negligible in comparison to NS .

The saddle point ($i\bar{\alpha} = \bar{a} > 0$, $l' = \bar{\sigma}$) determined by the equations (16) and (17) is the point of maximum of the function $s(i\alpha, l)$ on the integration contour shown in Fig. 2 as the quadratic form $\delta^2 s$ at this point is negative:

$$\begin{aligned} \delta^2 s(i\alpha = \bar{a}, l' = \bar{\sigma}) \\ = -(l - \bar{\sigma})^2 (l' - \bar{\sigma})^2 - (\bar{\sigma}^2 - \bar{\sigma}^2)(\text{Re}\alpha)^2 \leq 0, \end{aligned} \quad (21)$$

where $\bar{\sigma}^2 = \int d\tilde{\sigma} f_{\sigma} \sigma^2$. As to uniqueness of the saddle point, equation (17) and the relation between $1/a$ and the pressure, eq.(24) below, show that a physically acceptable \bar{a} must lie on the negative imaginary axis so that solutions to the equation (16) should be sought for real positive a . Our numerical findings have shown no sign of two different real positive solutions to equation (16) and in what follows we will assume that the solutions presented for different l and D are unique.

Note that the method applied above for solving the PF integral essentially consists in making use of an explicit analytical representation of the singular functions that determine the integration domain first in δx and y , then in δy , and finally in σ . In Appendix A, I show however that integration order over coordinates and the quantity fixing the integration domain, e.g., L' or L , is important and changing it has to be made with circumspection.

THE PRESSURES

The q1D system is anisotropic and has two different pressures: the longitudinal,

$$P_L = T(\partial S/\partial l)_D/D, \quad (22)$$

and the transverse

$$P_D = T(\partial S/\partial D)_l/l. \quad (23)$$

The l differentiation in (22) can be readily performed. The derivative $\partial \bar{\sigma}/\partial l$ can be computed as the l derivative

of the r.h.s. of equation (16). After a simple algebra one obtains:

$$P_L = \frac{T}{D(l - \bar{\sigma})}. \quad (24)$$

The D differentiation in (23) can also be readily obtained. Regarding for the relation (1) between σ_m , Δ , and D , one obtains

$$P_D = \frac{T \exp\left(-\frac{\sigma_m}{l - \bar{\sigma}}\right)}{ld \int_{\sigma_m}^1 \frac{d\sigma \sigma e^{-\frac{\bar{a}\sigma}{\sqrt{1-\sigma^2}}}}{\sqrt{1-\sigma^2}}}. \quad (25)$$

If the length per disk is replaced by the linear density $\rho = N/L = 1/l$, the pressures can be expressed as functions of ρ :

$$P_L = \frac{\rho T}{D(1 - \rho \bar{\sigma})}, \quad (26)$$

$$P_D = \frac{\rho T \exp\left(-\frac{\rho \sigma_m}{1 - \rho \bar{\sigma}}\right)}{d \int_{\sigma_m}^1 \frac{d\sigma \sigma e^{-\frac{\bar{a}\sigma}{\sqrt{1-\sigma^2}}}}{\sqrt{1-\sigma^2}}}.$$

These are remarkably simple formulas. While anticipating the form of P_D from the general ideas is hardly possible, the formula for P_L is very natural and could be expected from the starting expression for the PF (9). The PF of a one-dimensional HD system obtained by Tonks is $(L - Nd)^N$ and the pressure, in our notations, is $\sim (l - d)^{-1}$. But the formula (9) is the value of $(L - \sum \sigma)^N$ averaged over the distribution of σ and can be expected to give something like $(L - N\bar{\sigma})^N \propto (l - \bar{\sigma})^N$ so that P_L is naturally expected to scale as $(l - \bar{\sigma})^{-1}$ which is indeed the exact result (24). Moreover, in two limiting cases of a very small density and density at the close packing, the pressure along the pore has to coincide with the modified Tonks result $P_L \sim (l - \sigma_m)^{-1}$ in which d is replaced with the minimum possible distance along the pore. Indeed, in the former limit, it is because the pressure must scale as $1/l$; in the last limit, it is because the motion across the pore is fully hindered so that σ_m plays the role of d . The pressure in the form (24) naturally satisfies these requirements.

The quantity $\bar{\sigma}$ is a smooth function of both density ρ and thickness D . In particular, $\bar{\sigma} \rightarrow d$ as D goes to zero. Then the pressure P_L is an analytical function of ρ up to the close packing density $\rho = 1/\sigma_m$. This shows that the virial expansion of P_L does exist and converges to the exact pressure for all $\rho < 1/\sigma_m$. In particular, the virial series times D converges to the 1D pressure. Similarly, the transverse pressure P_D can also be expanded in a power series of ρ which is convergent up to the close packing density. The virial expansion of P_D though has not been considered so far.

The expressions for P_L and P_D which are similar in their form to our results (24) and (25) were obtained by Wojciechowski and coworkers in Ref.[8] in which the

PF was also derived by finding a stationary point of some functional. The direct comparison with our result is however difficult as these authors considered a q1D system periodic in the y direction. Moreover, there is a more substantial difference between this and our approach which is addressed in Appendix A.

Distribution of disks' centers across the pore.

We show here that the function f_σ (18) gives the probability distribution of contact distances σ along the pore hence equation (16) gives its mean value $\bar{\sigma}$. Clearly, in view of the relation (1), f_σ also determines the distribution of δy which is the difference between the y coordinates of two neighbors. We can also derive an analytical formula for the distribution function of y , the coordinates of disks' centers across the pore f_y . This probability distribution is the mean value of the y coordinate of a single disk, say disk k , i.e., $\langle \delta(y - y_k) \rangle$. To find it, we fix the transverse coordinate of k -th disk, $y_k = y > 0$, and separate the δy integrals over δy_{k-1} and δy_k from the rest $N - 3$ y integrals in formula (9):

$$\begin{aligned} \langle \delta(y - y_k) \rangle &\propto \int_{-\Delta}^{\Delta} D^{N-1} \delta y \delta(y - y_k) \\ &= \left[\int_{-\Delta/2-y}^{\Delta/2-y} d(y - y_{k-1}) \int_{-\Delta/2-y}^{\Delta/2-y} d(y_{k+1} - y) \right] \\ &\quad \times \int_{-\Delta}^{\Delta} D^{N-3} \delta y. \end{aligned} \quad (27)$$

Changing to the integration over σ , this reads

$$\int_{\sigma_m}^1 D^{N-1} \tilde{\sigma} \delta(y - y_k) = \int_{\sigma_m}^1 D^{N-3} \tilde{\sigma} \times I_k I_{k-1}, \quad (28)$$

where

$$I_k = \left[\int_{\sqrt{1-(y-\Delta/2)^2}}^1 d\tilde{\sigma}_{k-1} + \int_{\sqrt{1-(y+\Delta/2)^2}}^1 d\tilde{\sigma}_{k-1} \right]. \quad (29)$$

Next we separate terms in the delta function in (12) that depend on σ_{k-1} and σ_k ; the sum $\sum \sigma$ is not affected as removing two links of finite length out of $N - 1$ links is negligible in the thermodynamic limit. The probability of k -th disk to stay at y is proportional to the PF in the form given in (11) where $\int_{\sigma_m}^1 D^{N-1} \tilde{\sigma}$ is replaced by (28). As in such expression the only y dependent terms are $I_k I_{k-1} \exp(-a\sigma_k - a\sigma_{k-1})$, we conclude that the distri-

bution function of y normalized on unity is of the form

$$f_y(y) = \left[\int_{\sqrt{1-(y-\Delta/2)^2}}^1 \frac{\sigma e^{-\bar{a}\sigma} d\sigma}{\sqrt{1-\sigma^2}} + \int_{\sqrt{1-(y+\Delta/2)^2}}^1 \frac{\sigma e^{-\bar{a}\sigma} d\sigma}{\sqrt{1-\sigma^2}} \right] \times \frac{1}{A}, \quad (30)$$

$$A = \int_{-\Delta/2}^{\Delta/2} dy f_y A.$$

Here \bar{a} depends on l and D as the solution of equation (16). As this expression is symmetric with respect to the sign of y , there is no need to consider the case $y < 0$ separately.

In a similar way, one can show that the function f_σ (18) with $a = \bar{a}$ is the distribution function of σ . This probability distribution is the mean value of σ for some k , i.e., $\langle \delta(\sigma - \sigma_k) \rangle$. We fix σ_k at σ in the integrand of the integral over σ_k in (9) which gives the expression in the nominator of formula (18). Normalizing on unity, one obtains $\langle \delta(\sigma - \sigma_k) \rangle = f_\sigma$. Both analytically obtained distribution functions $f_\sigma(\sigma)$ and $f_y(y)$ will be presented below for different parameters of the pore.

PRESSURE AND DISKS' ARRANGEMENT IN THE PORE

The pressures along and across the pore as functions of the linear density $\rho = N/L$ are presented for three different pore widths: $\Delta = 0.141$ close to the 1D case, 0.5, and $\sqrt{3}/2 \approx 0.866$, the maximum width in the q1D system; the quantities P_L and P_D are shown in Fig.3 where also presented is the contribution of the term $1/D(l - \sigma_m)$. Consider the transverse pressure P_D . We see that for low densities this pressure is higher than the one along the pore. This is because in that case P_L is determined by a large x disks' separation whereas P_D is determined by a short range of y motion which is bounded from above by Δ . At sufficiently high density however the x separation becomes comparable with Δ and the two pressures may intersect. The disks' separation $l - \bar{\sigma}$ along x is $1/(P_L D)$. At the crossing points in Figs.3a and 3b one finds that for $\Delta = 0.141$, $l - \bar{\sigma} = 0.13$, and for $\Delta = 0.5$, $l - \bar{\sigma} = 0.33$ which are slightly lower than the correspondent Δ 's. This difference is because the disks mountain one upon another thereby decreasing the range of y motion and the stronger so the wider the pore is. This qualitatively explains why the difference between Δ and $l - \bar{\sigma}$ at the pressure crossing point increases with the pore width. For higher Δ , this effect is so strong that disks' y motion is highly restricted by their next neighbors and, e.g., for $\Delta = 0.86$ the transverse pressure is always above the longitudinal one. Both P_L and P_D tend to the curve $1/(l - \sigma_m)D$ in the close packing density limit as it should

be. Some more delicate peculiarities of the pressure behavior are related with the appearance of certain defects in the zigzag structure and will be discussed below in the Discussion.

The function $f_\sigma(\sigma)$ (18) with $a = \bar{a}$ presents the distribution of the longitudinal contact distances σ , eq.(1), and eq.(16) gives its mean value $\bar{\sigma}$. This $\bar{\sigma}$ is growing with l and for $l \sim 3$ practically attains its maximum limiting value $\bar{\sigma}_\infty = \bar{\sigma}(l \rightarrow \infty)$. The limiting value $\bar{\sigma}_\infty$ is larger for smaller Δ but remains below 1 for all $\Delta > 0$ ($\bar{\sigma}_\infty = 0.853, 0.956, 0.995$ for $\Delta = 0.866, 0.5, 0.141$ respectively), and only for $\Delta = 0$, i.e., in the 1D case, $\bar{\sigma} = \bar{\sigma}_\infty = 1$. This shows that the piecewise discontinuity in l' at the upper l' integration limit l'_{\max} in (14) is never attained and thus does not manifest itself.

The distributions $f_\sigma(\sigma)$ for $\Delta = 0.141, 0.5, 0.866$ is shown in Fig.4 for different densities $\rho = N/L$. Consider first f_σ for the case $\Delta = 0.5$, Fig.4.b, recently studied numerically by Huerta et al [14, 15]. This σ distribution has an important peculiarity: it has two peaks, one at the smallest $\sigma = \sigma_m$ and another one at the largest $\sigma = 1$, and a flat minimum in between. At a large density σ_m dominates implying that disks contact the opposite walls making a solidlike zigzag. At the same time, $\sigma = 1$ indicates that some disks can move across the pore through windows between the zigzags, Fig. 5. The second peak appears quite sharply in terms of the density variation, but not abruptly: it is present for any ρ , Fig.6, but becomes barely visible at about $\rho \approx 1.111$ (inset in Fig.5b) and well developed at $\rho = 1.056$. For $\rho > 1.111$ the σ_m peak dominates, at $\rho \sim 1.056$ the $\sigma = 1$ peak becomes well visible, then it grows and for $\rho < 1$ becomes higher than σ_m peak. This implies that at $\rho \sim 1.06$ an appreciable fraction of the zigzag arrangement is replaced by strings of disks with close y 's. At lower $\rho < 1$, the σ distribution becomes wide which shows that at low ρ disks freely move between the walls as in an ideal gas. This picture is in a qualitative agreement with the numerical simulation results of Refs.[11, 14, 15]. The pair distribution function along the pore was found to have sharp peak at the contact distance σ_m at high density $\rho = 1.11$, then it widens and, for $\rho \approx 1.056$, develops second peak at the unit distance which then widens and becomes dominating for $\rho = 0.91$. The system behavior for $\Delta = 0.866$ is qualitatively similar to that of $\Delta = 0.5$. As for $\Delta = 0.141$, this width is so narrow and the positions at the wall and at the center are so close that both peaks are present for the density 1.005 extremely close to the dense packing limit 1.008.

Fig. 7 presents the distribution function f_y (30) of coordinates y across the pore. It is shown for three pore widths and different densities up to very high ones close to the maximum possible dense packing densities.

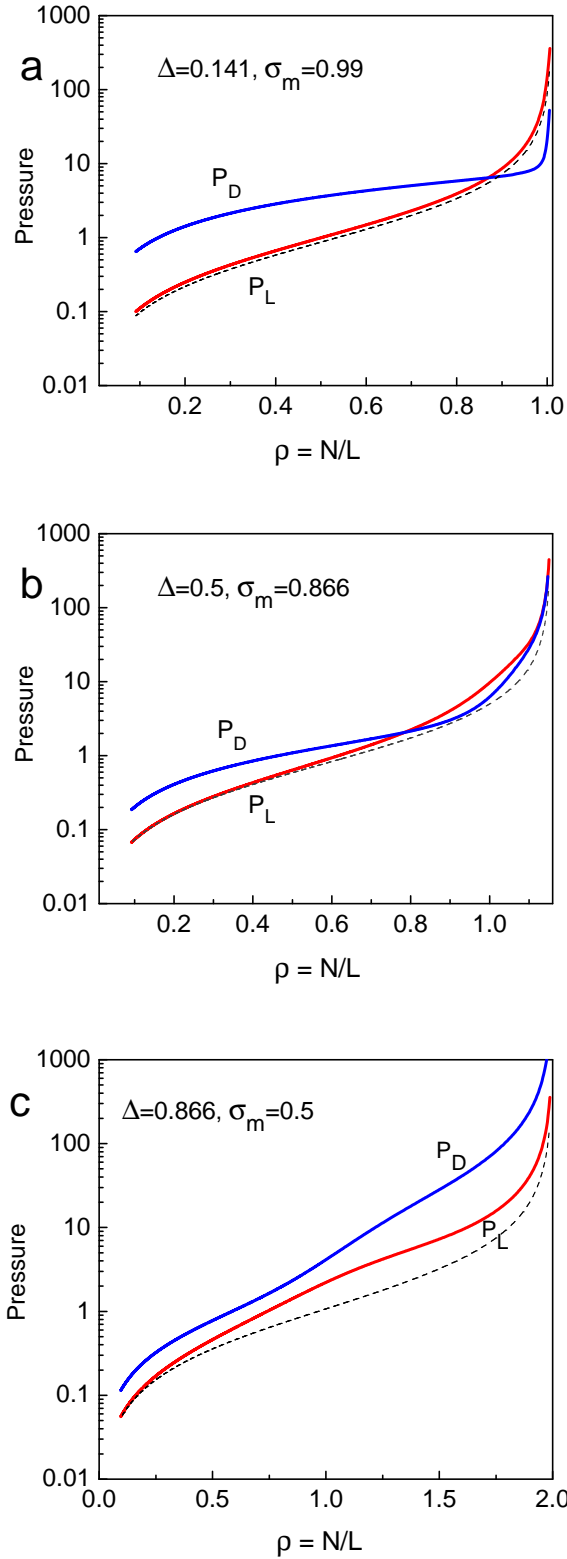


FIG. 3: The longitudinal, P_L , and transverse, P_D , pressures for three different widths Δ : a) 0.141, b) 0.5, c) 0.866. The dash curves show the contribution of the term $1/[D(l - \sigma_m)]$ with the relevant σ_m . T is set equal to 1. Note that, in Fig.3b, for large ρ the curve P_L lies above P_D so that there is no second crossing.

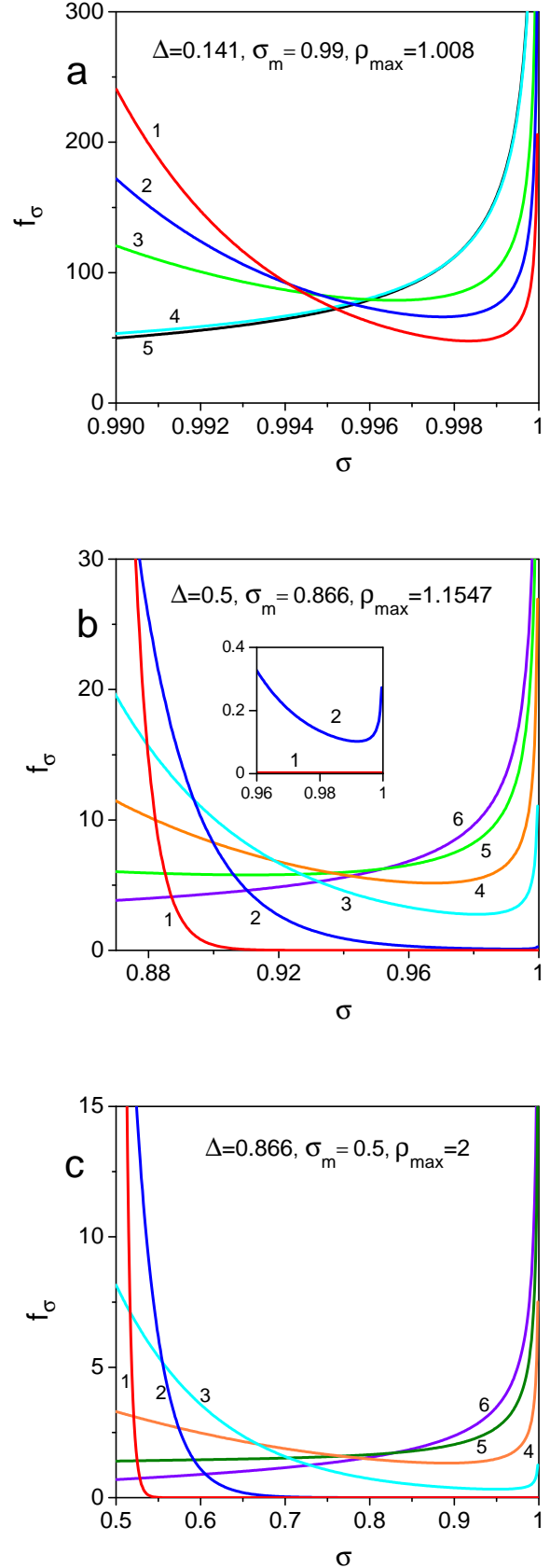


FIG. 4: The distribution f_σ of the contact distances σ in the condensates correspondent to three different widths Δ and various densities ρ : a) $\Delta=0.0141$: curve 1- $\rho=1.005$, 2-1.003, 3-1, 4-0.9, 5-0.091. b) $\Delta=0.5$: 1-1.14, 2-1.111, 3-1.056, 4-1.01, 5-0.79, 6-0.5. Inset: curves 1 and 2 near $\sigma=1$. c) $\Delta=0.866$: 1-1.96, 2-1.8, 3-1.4, 4-1.1, 5-0.8, 6-0.1.

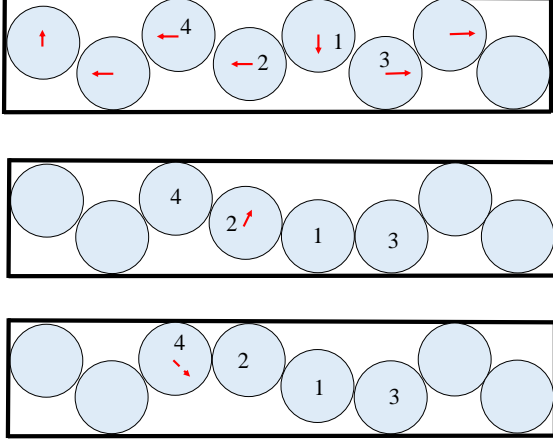


FIG. 5: Disks' rearrangement in a pore which creates a window for two disks to exchange their vertical positions. Upper panel: disk in the pore at the average distance along the pore which is below the diameter d and disks cannot exchange their vertical positions. To let disk 1 go down, disks on the left and right of it get more dense. Mid panel: disk 1 gets down through the window of size d between disks 2 and 3. Now disk 2 may get up between disks 4 and 1. Lower panel: the exchange of the vertical positions of disks 1 and 2 is accomplished. Now disk 4 potentially can move down.

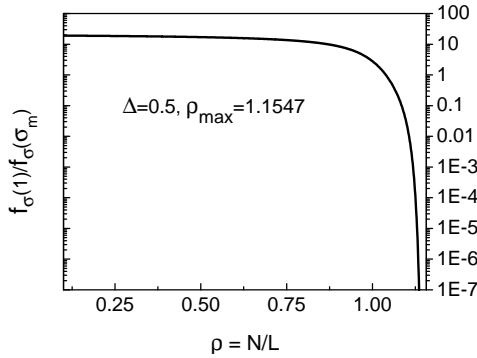


FIG. 6: Ratio $f_\sigma(\sigma = 1)/f_\sigma(\sigma = \sigma_m)$ as a function of the linear density ρ for $\Delta = 0.5$.

The 1D limit

It is important to see how the results obtained for a q1D system behave approaching a 1D system, i.e., in the limit $D \rightarrow 0$, when $\sigma_m \rightarrow 1$ ($\sigma_m \rightarrow d$) as $\Delta \rightarrow 0$. To this end, we first estimate the σ integral in this limit:

$$\int_{\sigma_m(\Delta)}^1 \frac{d\sigma \sigma e^{-\bar{a}\sigma}}{\sqrt{1-\sigma^2}} = e^{-\bar{a}\Delta} + O(\Delta^2). \quad (31)$$

Then the PF (20) goes over into the following expression:

$$Z(D \rightarrow 0) \approx (L - Nd)^N \Delta^N, \quad (32)$$

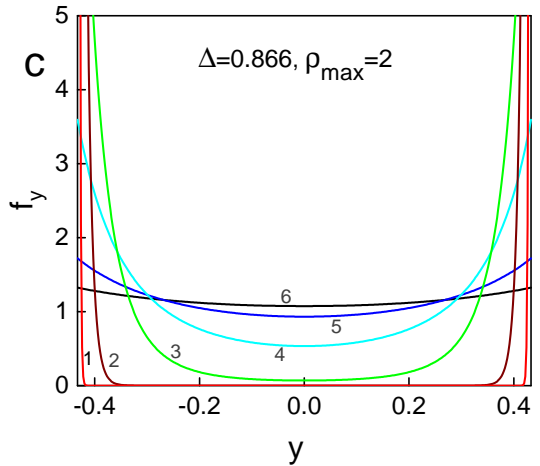
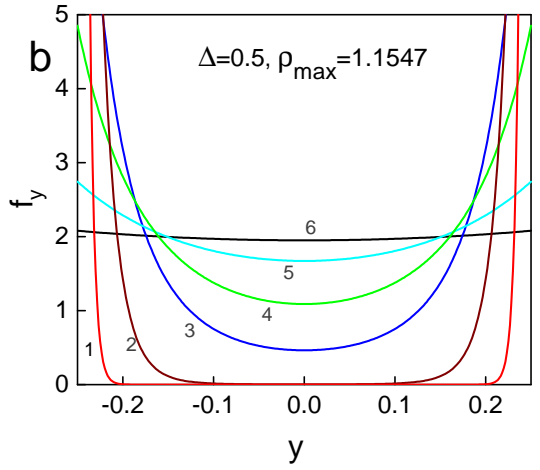
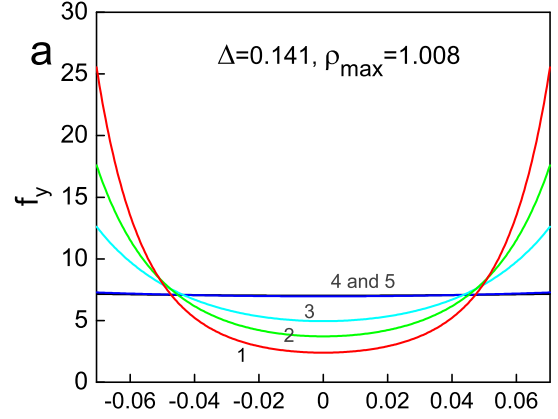


FIG. 7: The distribution function f_y of the disk coordinate y across the pore for three pore widths Δ and different densities ρ : a) $\Delta = 0.0141$: curve 1- $\rho=1.005$, 2-1.003, 3-1, 4-0.9, 5-0.8. b) $\Delta = 0.5$, 1-1.14, 2-1.111, 3-1.056, 4-1.01, 5-0.79, 6-0.5. c) $\Delta = 0.866$, 1-1.96, 2-1.8, 3-1.4, 4-1.1, 5-0.8, 6-0.5. ρ_{\max} is the maximum dense packing density.

which shows that in this limit the longitudinal and transverse degrees of freedom factorize. The longitudinal pressure times D in this limit recovers its 1D form $\propto T/(l-1)$ while the transverse pressure takes the form of that of an ideal gas in the volume Δd , $P_D = T\rho/\Delta d$. The inhomogeneous distribution f_y of the coordinates y across the pore in this limit behaves like

$$f_y \approx \frac{1 + \bar{a}\Delta^2\tilde{y}^2/2}{\Delta}, \quad (33)$$

where $0 \leq \tilde{y} \leq 1$. Thus, the inhomogeneity amplitude vanishes as pore width in power two. This is in line with the results of Refs.[17, 18] where similar dependence on the slit thickness was obtained by means of a perturbative approach to the transition from quasi 2D HD system in a slit to pure 2D HD system.

DISCUSSION

As we said above, a very small and extremely narrow peak at $\sigma = 1$ exists at any, even very large density, Figs.4,6. The above picture suggests that this peak is an essential part of the equilibrium state. At large ρ , but sufficiently decreased from the dense packing value, the disks choose to move closer to the walls to get compressed into solidlike zigzag array with the interparticle distance somewhat smaller than its average and σ smaller than $\bar{\sigma}$ in order to provide windows with σ close to unity (i.e., of size of the disk diameter), Fig.5. Through these windows the disks can interchange their vertical positions, extend their wondering to the total pore width and bring some entropy gain to the whole system. The two HDs in the window form a bound pair: the disks roll over each other's surface and their positions are highly correlated [19]. A local density increase needed to provide a window of size $\sigma = 1$ implies some increase of the pressure along the pore. At the same time, at such window the y range of disk motion should somewhat widen implying some decrease of transverse pressure. We interpret the slight upturn in P_L and slight downturn in P_D at ρ above $\rho = 1$ in Fig.3c as a manifestation of this effect: at the density 1.1, Fig.4c, the peak at $\sigma = 1$ becomes well developed implying that the number of $\sigma = 1$ windows is appreciable and can affect the pressures. As the density drops, the correlation between the disks weakens, the pair dissociates into free disks which can travel across the pore independently, their number rises while the number of HDs at the walls diminishes, Fig.6. This picture invokes similarity with a continuous Kosterlitz-Thouless transition from solidlike to liquidlike phase of a crystal. The similarity is supported by the numerical findings by Huerta et al [14, 15] that in the case $\Delta = 0.5$ above $\rho \sim 1.111$ the longitudinal pair correlation drops as a power law whereas below this ρ it drops exponentially. Thus, our theory shows that the crossover between the

solidlike zigzag and the liquidlike intermittence of zigzag and string arrangements is sharp in the scale of density variation, but continuous so that the thermodynamic potentials of a q1D system of HDs do not have discontinuities. The last conclusion is similar to that achieved by Varga et al [11] based on the numerical study of a q1D HD system. We emphasize that the narrow peak at $\sigma = 1$ for any density is the effect which can be lost in a finite system: only an infinite system can provide a window with $\sigma = 1$ for whatever density as its size is negligible in the limit $N \rightarrow \infty$.

CONCLUSION

Recently HDs in q1D geometry have received a great deal of interest and there is an indication that it will last. The transfer matrix method by Kofke and Post is on the way of incorporating wider pores where the interaction includes more than one next neighbor [20–23]. Moreover, HDs in q1D geometry are nowadays considered in a wider aspect related to glass transitions and HDs' dynamics [4, 14, 16, 24–26]. Our result gives the direct method to get the thermodynamics of a q1D HD system for given ρ, L, D which is required both for equilibrium and glassy states. The σ distribution (18) derived here suggests a novel quantitative analysis of the solidlike-to-liquidlike transformation and has already resulted in some new ideas [15]. The analytical formulas (24),(25) and (30) allow one to find the pressures along and across the system, disks' distribution across the pore, and pair correlations in a q1D HD system (the work is in progress) without the need to solve additional numerical problems. The result complements recent studies of low and high nonphysical dimensions which will hopefully advance our understanding of HD systems in the dimensions 2 and 3.

DATA AVAILABILITY STATEMENT

Data sharing is not applicable to this article as no new data were created or analyzed in this study.

Acknowledgment.

I am highly indebted to A. Trokhymchuk for numerous enlightening discussions. The work was supported by VC 202 from NAS of Ukraine and and NRFU Project 2020.01/0144.

Appendix A. Making use of analytical representations of singular functions and integration order in the statistical integrals

In HD systems, disks' coordinates are not independent and the integration limits are given by complex nontrivial

expressions. Making use of a step function θ in the statistical integrals with complicated integration limits is very convenient as it can formally simplify these limits so that the problem of solving the PF shifts to the integrating with singular functions. In this paper we demonstrated this in the case of a q1D HD system. In our integrals (4), (9), or (11) the arguments of the singular functions depend on the system length L and condensate length L' . Solving the PF, we enjoyed constant integration limits in the coordinates first integrating over the coordinates and then over L' . One may naturally ask if the order can be reversed. Moreover, there is often a need to integrate the expressions of the form (4), (9), or (11) with respect to the system length L , in particular, for Laplace's transform in L . The next extremely simple example shows that first integrating over L' or L and then over the coordinates can result in an inconsistency.

Consider the integral

$$I = \frac{1}{2} \int_0^L dL \int_0^1 dx \int_0^1 dy \theta(L - x - y). \quad (\text{A1})$$

This is an alternative expression for the integral

$$I = \int_0^L dL \int_0^L dx \int_0^{L-x} dy = L^3/6. \quad (\text{A2})$$

The reason for the form (A1) with the theta function is that it is convenient to deal with the *simple coordinate independent integration limits* in x and y . Consider I and, for simplicity, assume that $L \leq 1$ (the analytical results differ for $L < 1$ and $L > 1$). First integrating (A2) over xy and then over L gives the correct result:

$$I_{Lxy} = \int_0^L dL \int_0^L dx (L - x) = L^3/6. \quad (\text{A3})$$

This result can be reproduced by using θ function in the analytical form (5) and integrating (A1) in the same order:

$$\begin{aligned} I_{Lxy} &= \frac{1}{2} \int_0^L dL \int \frac{d\alpha}{2\pi i \alpha} e^{i\alpha L} \left(\frac{e^{-i\alpha L} - 1}{i\alpha} \right)^2 \\ &= \frac{1}{2} \int_0^L dL L^2 = L^3/6. \end{aligned} \quad (\text{A4})$$

Reversing the order in (A1) with theta function in the form (5) one gets:

$$I_{xyL} = \frac{1}{2} \int_0^1 dx \int_0^1 dy \int \frac{d\alpha}{2\pi i \alpha} \left[\frac{e^{i\alpha(L-x-y)}}{i\alpha} - \frac{e^{-i\alpha(x+y)}}{i\alpha} \right]. \quad (\text{A5})$$

The second term in the bracket gives zero as its exponent is negative. The first term has a pole of the second order

in α which gives

$$\begin{aligned} I_{xyL} &= \frac{1}{2} \int_0^1 dx \int_0^1 dy (L - x - y) \theta(L - x - y) \\ &= \frac{1}{2} \left(\int_0^L dx \int_0^{L-x} dy + \int_0^L dy \int_0^{L-y} dx \right) \\ &\times (L - x - y) \\ &= L^3/6 \end{aligned} \quad (\text{A6})$$

We see that the reverse order also gives the correct result, but if the integral was manifold, one would encounter a serious problem in integrating over the coordinates and here is why. If the L integration is performed *after* that over x and y , the integration limits in x and y are *independent* and the x, y integration is trivial, see (A4). In contrast, if the L integration is performed *before* that over x and y , the integration limits in x and y are *not independent* because of the presence of $\theta(L - x - y)$, see (A6). Thus, on the L integration one again arrives at the integral with coordinate dependent integration limits so that the goal has not been achieved: the integration over different coordinates cannot be performed independently. We emphasize that omitting $\theta(L - x - y)$ in (A7) does give an integral with constant integration limits but the result is incorrect:

$$\int_0^1 dx \int_0^1 dy (L - x - y) = L - 1 \leq 0! \quad (\text{A7})$$

Two remarks are now in order. First, the presence of the theta function after the L integration of PF of a HD system is general and not related to the specific form of the L integral. Second, if the integration over L is extended to infinity, the theta function must still be present as the integration from 0 to the maximum condensate length (in the above example it is 2) is included into it. In particular, the θ function will be present if Laplace's transformation of the PF has been made before the coordinate integration. In this case, to make the coordinate integrals all having the same integration limits, one has no choice but to disregard the theta function. However, as was shown above, omitting this function in the result of Laplace's transformation is incorrect. Hence incorrect would be the inverse Laplace's transformation, too.

Now we turn to the approach of Ref. [8]. To facilitate integration over coordinates, the authors first Laplace transform the PF and miss the theta function in the result. Due to this inconsistency, all the coordinate integrals have independent integration limits and thus factorize. As a consequence, some allowed points in the $N - 1$ dimensional coordinate space correspond to condensate's lengths exceeding the total length L (e.g., in our notations, all σ 's are equal to the disk diameter d whereas $L < (N - 1)d$). Next the inverse Laplace transformation is performed. However, the total contribution to this integral comes from the single maximum point

which can lie within the domain restricted by the missing theta function. Thus the intermediate inconsistency remains but, regarding for the expressions for pressures which are similar to (24) and (25), the result is correct. We emphasize that our approach is different from that of Ref. [8]. We have not used Laplace transformation and our success in performing the σ (coordinate) integrals is due to the representation (10) of the theta function in terms of a delta function.

* Electronic address: victorpergam@yahoo.com

- [1] J.-P. Hansen and I.R. McDonald, *Theory of simple liquids* (Academic, London 1986).
- [2] I.R. Yukhnovski and M.F. Holovko. *Statistical Theory of Classical Equilibrium Systems* (Naukova Dumka, Kyiv 1980) (in Russian).
- [3] *Theory and simulation of hard-sphere fluids and related systems*, edited by A. Mulero, Lect. Notes Phys. (Springer, Berlin 2008).
- [4] C. L. Hicks, M.J. Wheatley, M.J. Godfrey, and M.A. Moor, Phys. Rev. Lett. **120**, 225501 (2018).
- [5] P. Charbonneau, J. Kurchan, G. Parisi, P. Urbani, and F. Zamponi, Annu. Rev. Condens. Matter Phys. **8**, 265 (2017).
- [6] L. Tonks, Phys. Rev. **50**, 955 (1936).
- [7] J.A. Barker, Aust. J. Phys. **15** 127 (1962).
- [8] K.W. Wojciechowski, P. Pieranski, and J. Malecki, J. Chem. Phys. **76**, 6170 (1982).
- [9] D.A. Kofke and A.J. Post, J. Chem. Phys. **98**, 4853 (1993).
- [10] I.E. Kamenetskiy, K.K. Mon, and J.K. Percus, J. Chem. Phys. **121** 7355 (2004).
- [11] S. Varga, G. Balló, and P. Gurin, J. Stat. Mech. Theory Exp. P11006 (2011).
- [12] K.K. Mon, Phys. Rev. E **97**, 052114 (2018).
- [13] J.M. Kosterlitz and D.J. Thouless, J. Phys. C **6**, 1181(1973).
- [14] A. Huerta, T. Bryk, and A. Trokhymchuk, arXiv:1904.05970v1 (2019).
- [15] A. Huerta, T.M. Bryk, V.M. Pergamenschchik, and A.D. Trokhymchuk, Kosterlitz-Thouless-type caging-uncaging transition in a quazi-one dimensional hard disk system, Phys. Rev. Research **2**, 033351 (2020).
- [16] J.F. Robinson, M.J. Godfrey, and M.A. Moore, Phys. Rev. E **93**, 032101 (2016).
- [17] T. Franosch, S. Lang, and R. Schilling, Phys. Rev. Lett. **109**, 240601(2012).
- [18] S. Lang, T. Franosch, R. Schilling, J. Chem. Phys. **140**, 104506 (2014).
- [19] This exchanging event is also nicely illustrated graphically in [16].
- [20] M. Godfrey and M. Moore, Phys. Rev. E **91**, 022120 (2015).
- [21] P. Gurin and S. Varga, J. Chem. Phys. **142**, 224503 (2015).
- [22] P. Gurin, S. Varga, M. González-Pinto, Y. Martínez-Ratón, and E. Velasco, J. Chem. Phys. **146**, 134503 (2017).
- [23] Y. Hu, L. Fu, and P. Charbonneau, Mol. Phys. **116**, 3345 (2018).
- [24] M. Z. Yamchi, S. S. Ashwin, and R. K. Bowles, Phys. Rev. E **91**, 022301 (2015).
- [25] L. Fu, C. Bian, C. Wyatt Shields, D.F. Cruz, G..P. López, and P. Charbonneau, Soft Matter, **13**, 3296 (2017).
- [26] M. J. Godfrey and M. A. Moore, J. Stat. Mech. Theory Exper. (2020) 083303.